MODELING AND IDENTIFICATION OF A TWO-LINK FLEXIBLE MANIPULATOR

Jorge Augusto de Bonfim Gripp, jorge.gripp@gmail.com
Fábio L. M. Santos, fsantos@ita.br
Clayton Rodrigues Bernardo, claytonrb@gmail.com
Luiz Carlos Sandoval Góes, goes@ita.br
ITA - Instituto Tecnológico de Aeronáutica, Divisão de Engenharia Mecânica-Aeronáutica.
Praça Marechal Eduardo Gomes, 50 São José dos Campos/SP BRASIL 12228900

Abstract. In this work we study the modeling and identification of a two-link manipulator with mechanical flexibility distributed along the links. The experimental apparatus studied is a two-link flexible manipulator moving in the horizontal plane driven by two brushless DC motors. Experimental data collected is used for system identification. A finite dimensional model is derived using the assumed modes method. Lagrangian approach leads to explicit equations of motion. Actuators and sensors are also modeled in order to derive a complete and explicit model of the complete system.

Keywords: Modeling, Identification, Flexible robots

1. INTRODUCTION

The standard assumption that robotic manipulators consist only of rigid bodies is valid only for slow motion and small interacting forces. If flexibility is not taken into account, a degradation of the overall expected performance of the robot motion typically occurs. Flexibility manifests itself as mechanical oscillations and static deflections, greatly complicating the motion control of a mechanical arm. If the time to settle the oscillations is significant relative to the cycle time of the overall task, flexibility will be a major consideration in the arm design (De Luca and Book, 2008).

In this work, we study the modeling and identification of a two-link manipulator with mechanical flexibility distributed along the links.

The experimental apparatus is a two-link flexible manipulator driven by two brushless DC motors and monitored by tachometers, strain gauges, and accelerometers. A pneumatic system provides a frictionless cushion of air below the manipulator that moves in the horizontal plane. Both motors are excited with uncorrelated chirp signals and the experimental data is obtained through a setup with dSPACE hardware and software, together with MATLAB - Simulink.

From the modeling point of view the joint motion between the two links is separated into two inertias, each of them clamped in one link, in contrast to the conventional modeling that considers only one inertia fixed in the previous link as in De Luca and Siciliano (1991) and Lee and Lee (2002). Each flexible link is considered hybrid, containing rigid segments at its extremities.

The assumed modes method is adopted in order to obtain a finite-dimensional model that includes additional generalized coordinates that describe the elastic deflections. The Lagrangian approach is used to derive the dynamic model of the robotic structure. Explicit equations of motion are detailed assuming five shape functions for each link. Actuators and sensors are also modeled in order to derive a complete and explicit model of the whole system.

Furthermore, parametric system identification is done using experimental data. Theoretical and experimental results are compared to verify the accuracy of the model. The theoretical frequency response functions are evaluated using MATLAB software.

The paper is organized as follows: Section 2 gives the kinematic description for a planar two-link flexible manipulator. Kinetic and Potential energies are derived in Section 3 and the Lagrangian formulation is applied. Explicit formulation of the inertia matrix, stiffness matrix, and shape functions are detailed in Appendix. Section 4 is devoted to the modeling of Actuators and sensors, presenting a state-space representation. Experimental and theoretical results are presented in Section 5. Conclusions are drawn in Section 6.

2. KINEMATIC MODELING

Consider a two-link flexible manipulator with rotary joints subject to bending deformation that moves on a planar surface as showed in Fig. 1. Each link is denoted by an index i, where i = 1, 2. Three coordinate systems are established: the inertial system (X, Y) and two moving systems (X_i, Y_i) associated to each link i. The rigid motion is described by the joint angles θ_i, while $y_i(x_i)$ denotes the transversal deflection of link i at abscissa x_i, $0 < x_i < l_i$, where l_i is the length of the flexible part of the link. The angle between the coordinates (X_2, Y_2) and (X, Y) is $\alpha_2 = \theta_1 + \theta_2 + y'_{1e}$, where $y'_{ie} = (\partial y_i / \partial x_i)\big|_{x_i = l_i}$ and we consider the approximation $\arctan y'_{ie} = y'_{ie}$.
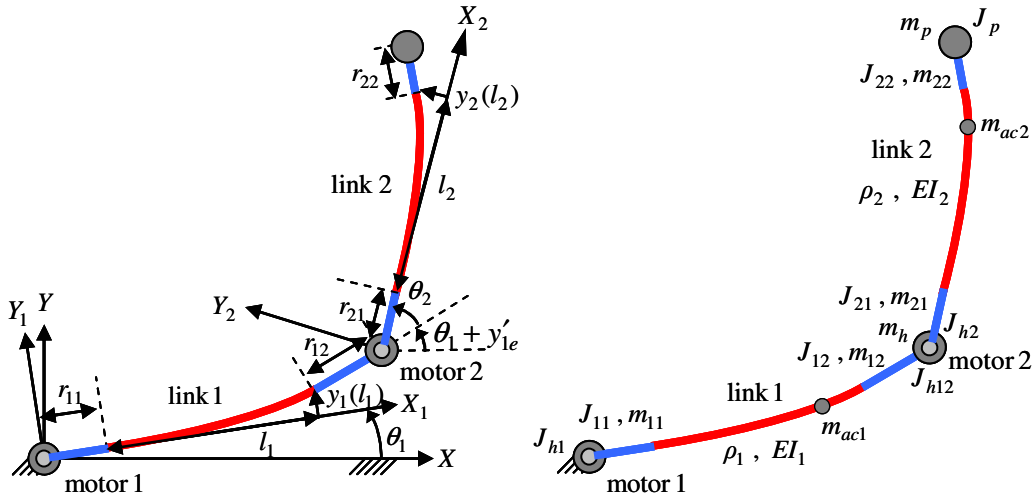
Figure 1. Geometric and Inertial parameters of the two-link flexible manipulator

Vector $^i\mathbf{p}_i = \begin{bmatrix} r_{i1} + x_i & y_i \end{bmatrix}^T$ represents a point along the flexible part of the link i with respect to coordinates (X_i, Y_i) and $\mathbf{p}_i = \begin{bmatrix} x & y \end{bmatrix}^T$ is the position the same point, but with respect to coordinates (X, Y) as in Eq. (1) and (3). Vector $\mathbf{p}_{ih}$ represents the end of the link i with respect to coordinates (X, Y) and is denoted in Eq. (2) and (4).

$$\mathbf{p}_1 = \mathbf{R}(\theta_1) \begin{bmatrix} r_{11} + x_1 \\ y_1(x_1) \end{bmatrix} \tag{1}$$

$$\mathbf{p}_{1h} = \mathbf{p}_1(l_1) + \mathbf{R}(\theta_1 + y'_{1e}) \begin{bmatrix} r_{12} \\ 0 \end{bmatrix} \tag{2}$$

$$\mathbf{p}_2 = \mathbf{p}_{1h} + \mathbf{R}(\alpha_2) \begin{bmatrix} r_{21} + x_2 \\ y_2(x_2) \end{bmatrix} \tag{3}$$

$$\mathbf{p}_{2h} = \mathbf{p}_{1h} + \mathbf{R}(\alpha_2) \begin{bmatrix} r_{21} + l_2 \\ y_2(l_2) \end{bmatrix} + \mathbf{R}(\alpha_2 + y'_{2e}) \begin{bmatrix} r_{22} \\ 0 \end{bmatrix} \tag{4}$$

$$\mathbf{R}(\theta) = \begin{bmatrix} \cos(\theta) & -\sin(\theta) \\ \sin(\theta) & \cos(\theta) \end{bmatrix} \tag{5}$$

Each link has two rigid segments on its extremities with constant linear density. The center of mass of each rigid segment is calculated as: $\mathbf{p}_{m11} = \tfrac{1}{2}\mathbf{p}_1(0)$, $\mathbf{p}_{m12} = \tfrac{1}{2}(\mathbf{p}_1(l_1) + \mathbf{p}_{1h})$, $\mathbf{p}_{m21} = \tfrac{1}{2}(\mathbf{p}_{1h} + \mathbf{p}_2(0))$, $\mathbf{p}_{m22} = \tfrac{1}{2}(\mathbf{p}_2(l_2) + \mathbf{p}_{2h})$.

From Eq. (1)-(5) is possible to derive the square of velocities denoted in Eq. (6)-(12), where $y_{ie} = y_i(l_i)$, $y_i = y_i(x_i)$. It was considered the approximations $x_i \gg y_i$ and $l_i \gg y_{ie}$ because the bending deformations are much smaller than the link length, i.e., second-order terms involving products of deformations where neglected.

$$\dot{\mathbf{p}}_1^T \dot{\mathbf{p}}_1 = \left((r_{11} + x_1)\dot{\theta}_1 + \dot{y}_1 \right)^2 \tag{6}$$

$$\dot{\mathbf{p}}_{1h}^T \dot{\mathbf{p}}_{1h} = \left((r_{11} + l_1)\dot{\theta}_1 + \dot{y}_{1e} + r_{12}(\dot{\theta}_1 + \dot{y}'_{1e}) \right)^2 \tag{7}$$

$$\dot{\mathbf{p}}_{m11}^T \dot{\mathbf{p}}_{m11} = \tfrac{1}{4} r_{11}^2 \dot{\theta}_1^2 \tag{8}$$

$$\dot{\mathbf{p}}_{m12}^T \dot{\mathbf{p}}_{m12} = \left((r_{11} + l_1)\dot{\theta}_1 + \dot{y}_{1e} + \tfrac{1}{2} r_{12}(\dot{\theta}_1 + \dot{y}'_{1e}) \right)^2 \tag{9}$$

$$\dot{\mathbf{p}}_2^T \dot{\mathbf{p}}_2 = \left((r_{11} + l_1)\dot{\theta}_1 + \dot{y}_{1e} + r_{12}(\dot{\theta}_1 + \dot{y}_{1e}') \right)^2 + \left((r_{21} + x_2)\dot{\alpha}_2 + \dot{y}_2 \right)^2 \\ + 2\left((r_{11} + l_1)\dot{\theta}_1 + \dot{y}_{1e} + r_{12}(\dot{\theta}_1 + \dot{y}_{1e}') \right)\left((r_{21} + x_2)\dot{\alpha}_2 + \dot{y}_2 \right)\cos(\theta_2) \tag{10}$$

$$\dot{\mathbf{p}}_{m21}^T \dot{\mathbf{p}}_{m21} = \left((r_{11} + l_1)\dot{\theta}_1 + \dot{y}_{1e} + r_{12}(\dot{\theta}_1 + \dot{y}_{1e}') \right)^2 + \left(\tfrac{1}{2} r_{21}\dot{\alpha}_2 \right)^2 + 2\left((r_{11} + l_1)\dot{\theta}_1 + \dot{y}_{1e} + r_{12}(\dot{\theta}_1 + \dot{y}_{1e}') \right)\left(\tfrac{1}{2} r_{21}\dot{\alpha}_2 \right)\cos(\theta_2) \tag{11}$$

$$\dot{\mathbf{p}}_{m22}^T \dot{\mathbf{p}}_{m22} = \left((r_{11} + l_1)\dot{\theta}_1 + \dot{y}_{1e} + r_{12}(\dot{\theta}_1 + \dot{y}_{1e}') \right)^2 + \left((r_{21} + l_2)\dot{\alpha}_2 + \dot{y}_{2e} + \tfrac{1}{2} r_{22}(\dot{\alpha}_2 + \dot{y}_{2e}') \right)^2 \\ + 2\left((r_{11} + l_1)\dot{\theta}_1 + \dot{y}_{1e} + r_{12}(\dot{\theta}_1 + \dot{y}_{1e}') \right)\left((r_{21} + l_2)\dot{\alpha}_2 + \dot{y}_{2e} + \tfrac{1}{2} r_{22}(\dot{\alpha}_2 + \dot{y}_{2e}') \right)\cos(\theta_2) \tag{12}$$

3. LAGRANGIAN MODELING

Lagrangian mechanics is a re-formulation of classical mechanics that uses conservation of energy. In Lagrangian mechanics, the equations of motion of a system of particles are derived by solving the Lagrange equations. The kinetic energy T and potential energy V are computed to calculate the Lagrangian $L = T - V$ (Lemos, 2004).

The kinetic energy of the two-link flexible manipulator in Fig. 1 the sum of the following contributions:

$$T = T_b + \sum_{i=1}^{2}\sum_{j=1}^{2} T_{ij} + \sum_{i=1}^{2} T_i + T_h + T_p + \sum_{i=1}^{2} T_{aci} \tag{13}$$

The kinetic rotational energy of the rigid body of moment of inertia J_{h1} located at the basis is:

$$T_b = \frac{1}{2} J_{h1}\dot{\theta}_1^2 \tag{14}$$

The kinetic energy of the rigid segments of the links in Eq. (15) depends on the moment of inertia of the rigid segment J_{ij} and the mass of the segment m_{ij}. Each segment has a constant linear density ρ_{ij} along the segment.

$$T_{ij} = \frac{1}{2} m_{ij}\left(\dot{\mathbf{p}}_{mij}^T \dot{\mathbf{p}}_{mij} \right) + \frac{1}{2} J_{ij}\sigma_{ij}^2 \tag{15}$$

Where $\sigma_{11} = \dot{\theta}_1$, $\sigma_{12} = \dot{\theta}_1 + \dot{y}_{1e}'$, $\sigma_{21} = \dot{\alpha}_2$ e $\sigma_{22} = \dot{\alpha}_2 + \dot{y}_{2e}'$. The kinetic energy of the rigid bodies located between the links in Eq. (16) depends on the moment of inertia of the body clamped at the first link J_{h12}, the body clamped at the second link J_{h2} and the sum of the bodies mass m_h.

$$T_h = \frac{1}{2} m_h\left(\dot{\mathbf{p}}_{1h}^T \dot{\mathbf{p}}_{1h} \right) + \frac{1}{2} J_{h12}\left(\dot{\theta}_1 + \dot{y}_{1e}' \right)^2 + \frac{1}{2} J_{h2}\dot{\alpha}_2^2 \tag{16}$$

Where $\dot{y}_{ie}' = \frac{d}{dt}\left((\partial y_i / \partial x_i)\big|_{x_i = l_i} \right)$. The kinetic energy of the payload m_p at the tip of second link is:

$$T_p = \frac{1}{2} m_p\left(\dot{\mathbf{p}}_{2h}^T \dot{\mathbf{p}}_{2h} \right) + \frac{1}{2} J_p\left(\dot{\alpha}_2 + \dot{y}_{2e}' \right)^2 \tag{17}$$

The kinetic energy of the flexible link i with linear density ρ_i is:

$$T_i = \frac{1}{2} \int_0^{l_i} \rho_i\left(\dot{\mathbf{p}}_i^T \dot{\mathbf{p}}_i \right) dx_i \tag{18}$$

We consider also the kinetic translational energy of each accelerometer with mass m_{aci} positioned at $x_i = l_{aci}$:

$$T_{aci} = \frac{1}{2} m_{aci}\left(\dot{\mathbf{p}}_i^T \dot{\mathbf{p}}_i \right)\bigg|_{x_i = l_{aci}} \tag{19}$$

The potential energy of the system is due to the elastic potential of each flexible link i with elastic modulus E and second moment of area density I_i. No gravitational potential energy is considered because the system moves on the horizontal plane.

$$V = \sum_{i=1}^{2} \frac{1}{2} \int_0^{l_i} EI_i \left(\frac{\partial^2 y_i(x_i,t)}{\partial x_i^2} \right)^2 dx_i \tag{20}$$

The assumed modes method is adopted in order to obtain a finite-dimensional model that includes additional generalized coordinates that describe the elastic deflections $y_i(x_i,t)$. The deflection is separate in time and space:

$$y_i(x_i,t) = \sum_{j=1}^{n_i} \phi_{ij}(x_i)\delta_{ij}(t) \tag{21}$$

We consider $n_1 = 5$ modes for the first link and $n_2 = 5$ modes for the second link. Defining $\mathbf{\Phi}_1 = [\phi_{11},...,\phi_{1n_1}]^T$, $\mathbf{\Phi}_2 = [\phi_{21},...,\phi_{2n_2}]^T$, $\mathbf{g}_1 = [\delta_{11},...,\delta_{1n_1}]^T$, and $\mathbf{g}_2 = [\delta_{21},...,\delta_{2n_2}]^T$, Eq. (21) becomes Eq. (22). The shape equations $\mathbf{\Phi}_1$ and $\mathbf{\Phi}_2$ are calculated in Appendix.

$$y_i(x_i,t) = \mathbf{\Phi}_i^T(x_i)\mathbf{g}_i(t) \tag{22}$$

The formula of the Lagrangian $L = T - V$ is derived from Eq. (6)-(20) and (22) as a function of a vector of generalized coordinates $\mathbf{q} = \begin{bmatrix} \theta_1 & \theta_2 & \mathbf{g}_1^T & \mathbf{g}_2^T \end{bmatrix}^T = \begin{bmatrix} \theta_1 & \theta_2 & \delta_{11} & ... & \delta_{1n_1} & \delta_{21} & ... & \delta_{2n_2} \end{bmatrix}^T$.

Equation (23) is the Lagrange equation or Euler-Lagrange equation.

$$\frac{d}{dt}\left(\frac{\partial L}{\partial \dot{\mathbf{q}}} \right)^T - \left(\frac{\partial L}{\partial \mathbf{q}} \right)^T = \mathbf{f} \tag{23}$$

Where $\mathbf{f} = \begin{bmatrix} \tau_1 & \tau_2 & 0 & 0 & 0 & 0 \end{bmatrix}^T$ is the vector of generalized forces on the system.

As result of the Lagrangian approach, Eq. (23) derives the equations of motion (24), where $\mathbf{M}$ is the inertia matrix, $\mathbf{h}$ is the Coriolis vector and centrifugal forces, and $\mathbf{K}$ is the stiffness matrix as calculated in the Appendix.

$$\mathbf{M}(\mathbf{q})\ddot{\mathbf{q}} + \mathbf{h}(\mathbf{q},\dot{\mathbf{q}}) + \mathbf{K}\mathbf{q} = \mathbf{f} \tag{24}$$

4. ACTUATORS AND SENSORS MODELING

The generalized forces vector $\mathbf{f}$ presented in Eq. (23) is a function of the actuator torque in the joint of the basis (τ_1) and in the joint between the two links (τ_2). Each actuator is a DC electric motor as showed in Fig. 2. Sensor modeling intends to present $\mathbf{f}$ as a function the input vector $\mathbf{u} = \begin{bmatrix} e_1 & e_2 \end{bmatrix}^T$.
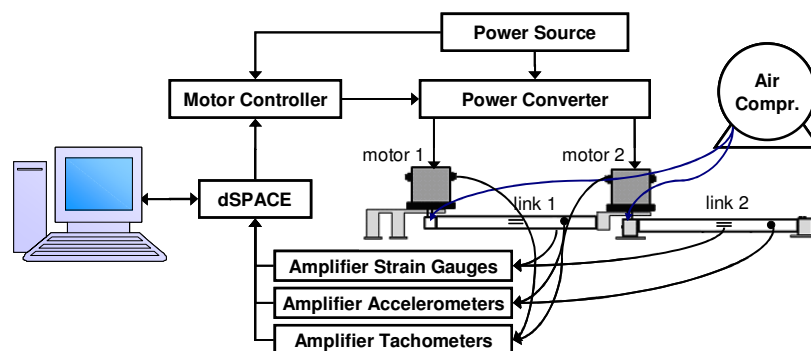

Figure 2. Experimental setup

Each motor has a controller and each controller can be set at "torque mode". At torque mode, the voltage signal e_i provided by dSPACE is converted into a proportional current signal i_{ai}. The torque generated by the DC motor τ_m is proportional to the armature current i_{ai}, i.e. τ_m is proportional to the input voltage e_i, where k_t is the motor torque constant:

$$\tau_m = k_t e_i \tag{25}$$

The resulting torque τ_i is computed excluding the torque friction, where c_v is the friction constant:

$$\tau_i = \tau_m - c_v \dot{\theta}_m \tag{26}$$

From Eq. (25)-(26) it is possible to define τ_i as function of e_i and $\dot{\theta}_i$, where $i = 1, 2$.

$$\tau_i = k_t e_i - c_v \dot{\theta}_i \tag{27}$$

Using Eq. (27) it is possible to define $\mathbf{f}$ as function of $\mathbf{u}$ and Equation (24) can be rewritten as:

$$\mathbf{M(q)\ddot{q} + P\dot{q} + Kq + h(q,\dot{q}) = Qu} \tag{28}$$

$$\mathbf{Q} = k_t \begin{bmatrix} \mathbf{I}_2 \\ \mathbf{0}_{(n_1+n_2)\times 2} \end{bmatrix}, \quad \mathbf{P} = c_v \begin{bmatrix} \mathbf{I}_2 & \mathbf{0}_{2\times(n_1+n_2)} \\ \mathbf{0}_{(n_1+n_2)\times 2} & \mathbf{0}_{(n_1+n_2)\times(n_1+n_2)} \end{bmatrix} \tag{29}$$

Where $\mathbf{I}_n$ is the $n \times n$ identity matrix and $\mathbf{0}_{m\times n}$ is the $m \times n$ zero matrix. We define the state vector $\mathbf{x}$ and the output vector $\mathbf{y}$ in Eqs. (30)-(31). Figure 3 shows the input vector $\mathbf{u}$ (two chirp signals) and the output vector $\mathbf{y}$.

$$\mathbf{x} = \begin{bmatrix} \mathbf{q} \\ \dot{\mathbf{q}} \end{bmatrix} = \begin{bmatrix} \theta_1 & \theta_2 & \delta_{11} & \ldots & \delta_{1n_1} & \delta_{21} & \ldots & \delta_{2n_2} & \dot{\theta}_1 & \dot{\theta}_2 & \dot{\delta}_{11} & \ldots & \dot{\delta}_{1n_1} & \dot{\delta}_{21} & \ldots & \dot{\delta}_{2n_2} \end{bmatrix}^T \tag{30}$$

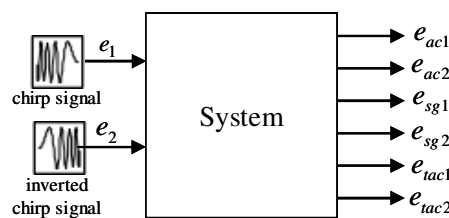$$\mathbf{y} = \begin{bmatrix} e_{ac1} & e_{ac2} & e_{sg1} & e_{sg2} & e_{tac1} & e_{tac2} \end{bmatrix}^T \tag{31}$$

Figure 3. Inputs and outputs of the system

Linearization of Eq. (28) around $\mathbf{q} = \mathbf{0}$ leads $\mathbf{M(q)} = \mathbf{M}_a + \mathbf{M}_b \cos(\theta_2)$ becomes $\mathbf{M} = \mathbf{M}_a + \mathbf{M}_b$ and $\mathbf{h(q,\dot{q})} = \mathbf{h}_a(\mathbf{q},\dot{\mathbf{q}})\sin(\theta_2)$ becomes $\mathbf{h} = \mathbf{0}$. Equations (32)-(33) are the state-space representation, where $\mathbf{A}$ is the state matrix, $\mathbf{B}$ is the input matrix, $\mathbf{C}$ is the output matrix, and $\mathbf{D}$ is the feedforward matrix (Ogata, 2003).

$$\dot{\mathbf{x}} = \mathbf{Ax} + \mathbf{Bu} \tag{32}$$

$$\mathbf{y} = \mathbf{Cx} + \mathbf{Du} \tag{33}$$

$$\mathbf{A} = \begin{bmatrix} \mathbf{0}_{(2+n_1+n_2)\times(2+n_1+n_2)} & \mathbf{I}_{(2+n_1+n_2)} \\ -(\mathbf{M}_a + \mathbf{M}_b)^{-1}\mathbf{K} & -(\mathbf{M}_a + \mathbf{M}_b)^{-1}\mathbf{P} \end{bmatrix}, \quad \mathbf{B} = \begin{bmatrix} \mathbf{0}_{(2+n_1+n_2)\times 2} \\ (\mathbf{M}_a + \mathbf{M}_b)^{-1}\mathbf{Q} \end{bmatrix} \tag{34}$$

The output matrix $\mathbf{C}$ and the feedforward matrix $\mathbf{D}$ are shown in Eq. (39)-(40), where e_{aci} is the integral of the accelerometer output over time, e_{sgi} is the strain gage output, and e_{taci} is the tachometer output as in Eq. (34)-(37).

$$e_{ac1} = G_{ac1}\{(r_{11}+l_{ac1})\ddot{\theta}_1 + \ddot{y}_1(l_{ac1})\} \tag{35}$$

$$e_{ac2} = G_{ac2}\{(r_{11}+l_1)\ddot{\theta}_1 + \ddot{y}_1(l_1) + r_{12}(\ddot{\theta}_1 + \ddot{y}'_{1e}) + (r_{21}+l_{ac2})\ddot{\alpha}_2 + \ddot{y}_2(l_{ac2})\} \tag{36}$$

$$e_{sgi} = G_{sgi}\left(\partial^2 y_i / \partial x_i^2\right)\Big|_{x_i=l_{sgi}} \tag{37}$$

$$e_{taci} = G_{taci}\dot{\theta}_i \tag{38}$$

$$\mathbf{C} = \begin{bmatrix} G_{ac1}\left[(r_{11}+l_{ac1}) \quad 0 \quad \mathbf{\Phi}_1^T\big|_{l_{ac1}} \quad \mathbf{0}_{1\times n_2}\right]\left[-\mathbf{M}^{-1}\mathbf{K} \quad -\mathbf{M}^{-1}\mathbf{P}\right] \\ G_{ac2}\left[(r_{11}+l_1+r_{12}+r_{21}+l_{ac2}) \quad (r_{21}+l_{ac2}) \quad (r_{12}+r_{21}+l_{ac2})\mathbf{\Phi}'^T_{1e}\big|_{l_1}+\mathbf{\Phi}^T_{1e}\big|_{l_1} \quad \mathbf{\Phi}^T_2\big|_{l_{ac2}}\right]\cdot\left[-\mathbf{M}^{-1}\mathbf{K} \quad -\mathbf{M}^{-1}\mathbf{P}\right] \\ G_{sg1}\left[0 \quad 0 \quad \left(\partial^2\mathbf{\Phi}_1^T/\partial x_1^2\right)\big|_{x_1=l_{sg1}} \quad \mathbf{0}_{1\times n_2} \quad 0 \quad 0 \quad \mathbf{0}_{1\times n_1} \quad \mathbf{0}_{1\times n_2}\right] \\ G_{sg2}\left[0 \quad 0 \quad \mathbf{0}_{1\times n_1} \quad \left(\partial^2\mathbf{\Phi}_2^T/\partial x_2^2\right)\big|_{x_2=l_{sg2}} \quad 0 \quad 0 \quad \mathbf{0}_{1\times n_1} \quad \mathbf{0}_{1\times n_2}\right] \\ G_{tac1}\left[0 \quad 0 \quad \mathbf{0}_{1\times n_1} \quad \mathbf{0}_{1\times n_2} \quad 1 \quad 0 \quad \mathbf{0}_{1\times n_1} \quad \mathbf{0}_{1\times n_2}\right] \\ G_{tac2}\left[0 \quad 0 \quad \mathbf{0}_{1\times n_1} \quad \mathbf{0}_{1\times n_2} \quad 0 \quad 1 \quad \mathbf{0}_{1\times n_1} \quad \mathbf{0}_{1\times n_2}\right] \end{bmatrix} \tag{39}$$

$$\mathbf{D} = \begin{bmatrix} G_{ac1}\left[(r_{11}+l_{ac1}) \quad 0 \quad \mathbf{\Phi}_1^T\big|_{l_{ac1}} \quad \mathbf{0}_{1\times n_2}\right]\mathbf{M}^{-1}\mathbf{Q} \\ G_{ac2}\left[(r_{11}+l_1+r_{12}+r_{21}+l_{ac2}) \quad (r_{21}+l_{ac2}) \quad (r_{12}+r_{21}+l_{ac2})\mathbf{\Phi}'^T_{1e}\big|_{l_1}+\mathbf{\Phi}^T_{1e}\big|_{l_1} \quad \mathbf{\Phi}^T_2\big|_{l_{ac2}}\right]\mathbf{M}^{-1}\mathbf{Q} \\ \mathbf{0}_{4\times 2} \end{bmatrix} \tag{40}$$

Equations (32)-(33) derives frequency response functions $\mathbf{H}(s)$, where $s = j2\pi f$ is the complex angular frequency. Theoretical model frequency response functions $\mathbf{H}(s)$ are presented in Fig. 4.

$$\mathbf{H}(s) = \mathbf{C}(s\mathbf{I} - \mathbf{A})^{-1}\mathbf{B} + \mathbf{D} \tag{41}$$

5. EXPERIMENTAL RESULTS

The experimental apparatus is showed in Fig. 2. The frequency range desired was 0 to 70 Hz, enough to identify the two first vibration modes. Two uncorrelated chirp (sweep) signals are applied to the motors, one with increasing frequencies from 0 to 70 Hz and another decreasing from 70 to 0 Hz. Data is collected at 250 samples per second through a setup with dSPACE hardware and software, together with MATLAB and Simulink.

The Welch Method is used to estimate the power spectral density as in Ljung and Glad (1994). Each collected signal was divided in 40 segments with 50% overlap to smooth the curve and a Hamming window was used. This procedure is contained at MATLAB function "tfestimate", generating the experimental frequency response functions.

Geometric parameters were measured, but friction constants and inertial parameters were adjusted using parametric identification. The objective function is the quadratic error between theoretical and experimental graphs, not considering the bias (difference between the mean of theoretical and experimental graphs). Theoretical parameters were tuned minimizing the multivariable objective function using MATLAB function "fmincon". Identified theoretical and experimental frequency response functions of accelerometers, strain gages, and tachometers are compared in Fig. 4.
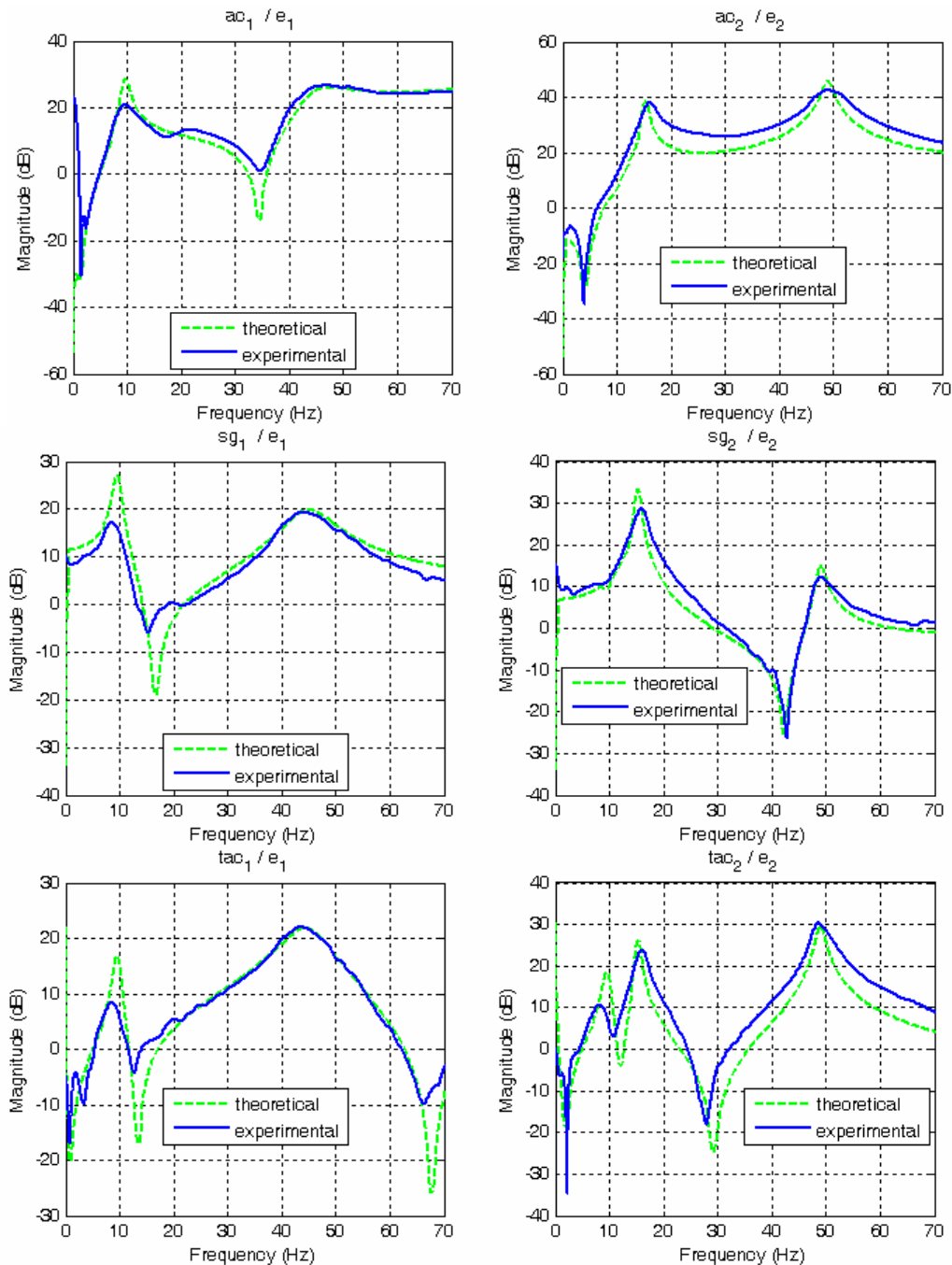
Figure 4. Theoretical and experimental frequency response functions of sensors

6. CONCLUSION

This paper presented the modeling and the parametric identification of a two-link manipulator with two flexible links. Dynamic model was derived based on Lagrangian approach assuming two modes of vibration for each link. Sensors and actuator were also modeled, deriving a complete set of dynamic equations of motion.

The rigid joint motion between the two links was separated into two inertias, in contrast to the conventional modeling that considers only one inertia fixed in the previous link. Rigid segments at extremities of the links were considered in order to improve the modeling. The mass of the acceleration sensors affects the system response and is also considered in the modeling.

The theoretical model has been simulated and compared to experimental results. Parametric identification successfully fit theoretical and experimental frequency response functions.

'7. ACKNOWLEDGEMENTS

8. REFERENCES

De Luca, A. and Book, W., 2008, "Robots with Flexible Elements", In: Siciliano, B. and Khatib, O., "Springer Handbook of Robotics", Springer, pp. 287-319.

De Luca, A. and Siciliano, B., 1991, "Closed-Form Dynamic Model of Planar Multilink Lightweight Robots", IEEE Transactions on Systems, Man and Cybernetics, v. 21, n. 4, p. 826-839.

Lee, S. and Lee, C., 2002, "Hybrid Control Scheme for Robust Tracking of Two-Link Flexible Manipulator", Journal of Intelligent and Robotic Systems, v. 34, n. 4, p. 431-452.

Lemos, N. A.,2004, "Mecânica Analítica", 1. ed. São Paulo: Editora Livraria da Física. v. 1. 386 p.

Ljung, L. and Glad, T., 1994, "Modeling Of Dynamic Systems", Part III – Identification, Prentice Hall, c8, pp. 191-226.

Ogata, K., 2003, "Engenharia de controle moderno", 4. ed., S.Paulo, Pearson Prentice Hall, 788p.

9. RESPONSIBILITY NOTICE

The authors are the only responsible for the printed material included in this paper.

APPENDIX

Matrices $\mathbf{M}$ and $\mathbf{K}$.

Equation (24) is expanded and its terms are calculated using Eq. (23):

$$\begin{bmatrix} M_{11} & M_{12} & \mathbf{M_{13}} & \mathbf{M_{14}} \\ M_{12} & M_{22} & \mathbf{M_{23}} & \mathbf{M_{24}} \\ \mathbf{M_{13}^T} & \mathbf{M_{23}^T} & \mathbf{M_{33}} & \mathbf{M_{34}} \\ \mathbf{M_{14}^T} & \mathbf{M_{24}^T} & \mathbf{M_{34}^T} & \mathbf{M_{44}} \end{bmatrix} \begin{bmatrix} \ddot{\theta}_1 \\ \ddot{\theta}_2 \\ \ddot{\mathbf{g}}_1 \\ \ddot{\mathbf{g}}_2 \end{bmatrix} + \begin{bmatrix} h_1 \\ h_2 \\ \mathbf{h_3} \\ \mathbf{h_4} \end{bmatrix} + \begin{bmatrix} 0 & 0 & \mathbf{0} & \mathbf{0} \\ 0 & 0 & \mathbf{0} & \mathbf{0} \\ \mathbf{0} & \mathbf{0} & \mathbf{K_{33}} & \mathbf{0} \\ \mathbf{0} & \mathbf{0} & \mathbf{0} & \mathbf{K_{44}} \end{bmatrix} \begin{bmatrix} \theta_1 \\ \theta_2 \\ \mathbf{g}_1 \\ \mathbf{g}_2 \end{bmatrix} = \begin{bmatrix} \tau_1 \\ \tau_2 \\ \mathbf{0} \\ \mathbf{0} \end{bmatrix}$$

$M_{11} = J_{11} + J_{12} + J_{21} + J_{22} + J_{h1} + J_{h12} + J_{h2} + J_p + J_{o1} + J_{o2} + m_{12}(l_1 + r_{11} + \tfrac{1}{2}r_{12})^2 + m_{ac1}(r_{11} + l_{1ac})^2$

$+ \tfrac{1}{4}m_{11}r_{11}^2 + (m_{21} + m_{22} + m_h + m_p + m_2)(l_1 + r_{11} + r_{12})^2 + \tfrac{1}{4}m_{21}r_{21}^2 + m_{22}(l_2 + r_{21} + \tfrac{1}{2}r_{22})^2 + m_1 r_{11}^2$

$+ m_p(l_2 + r_{21} + r_{22})^2 + 2m_1 d_1 r_{11} + m_2 r_{21}^2 + 2m_2 d_2 r_{21} + m_{21}(l_1 + r_{11} + r_{12})r_{21} + 2m_p(l_1 + r_{11} + r_{12})(l_2 + r_{21} + r_{22})$

$+ 2m_{22}(l_1 + r_{11} + r_{12})(l_2 + r_{21} + \tfrac{1}{2}r_{22}) + 2(l_1 + r_{11} + r_{12})(m_2 r_{21} + m_2 d_2) + m_{ac2}(r_{11} + l_1 + r_{12} + r_{21} + l_{ac2})^2$

$M_{12} = J_{21} + J_{22} + J_{h2} + J_p + J_{o2} + \tfrac{1}{4}m_{21}r_{21}^2 + m_p(l_2 + r_{21} + r_{22})^2 + m_{22}(l_2 + r_{21} + \tfrac{1}{2}r_{22})^2 + m_2 r_{21}^2 + 2m_2 d_2 r_{21}$

$+ \tfrac{1}{2}m_{21}(l_1 + r_{11} + r_{12})r_{21} + m_{22}(l_1 + r_{11} + r_{12})(l_2 + r_{21} + \tfrac{1}{2}r_{22}) + m_p(l_1 + r_{11} + r_{12})(l_2 + r_{21} + r_{22})$

$+ (l_1 + r_{11} + r_{12})(m_2 r_{21} + m_2 d_2) + m_{ac2}(r_{11} + l_1 + r_{12} + r_{21} + l_{ac2})(r_{21} + l_{ac2})$

$\mathbf{M_{13}} = (J_{12} + J_{21} + J_{22} + J_{h12} + J_{h2} + J_p + J_{o2})\mathbf{\Phi}_{1e}'^T + m_{ac2}(r_{11} + l_1 + r_{12} + r_{21} + l_{ac2})(\mathbf{\Phi}_{1e}^T + (r_{12} + r_{21} + l_{ac2})\mathbf{\Phi}_{1e}'^T)$

$+ (m_p(l_2 + r_{21} + r_{22})^2 + m_{22}(l_2 + r_{21} + \tfrac{1}{2}r_{22})^2 + m_2 r_{21}^2 + 2m_2 d_2 r_{21})\mathbf{\Phi}_{1e}'^T + m_{12}(l_1 + r_{11} + \tfrac{1}{2}r_{12})(\mathbf{\Phi}_{1e}^T + \tfrac{1}{2}r_{12}\mathbf{\Phi}_{1e}'^T)$

$+ (m_{21} + m_{22} + m_h + m_p + m_2)(l_1 + r_{11} + r_{12})(\mathbf{\Phi}_{1e}^T + r_{12}\mathbf{\Phi}_{1e}'^T) + \tfrac{1}{4}m_{21}r_{21}^2\mathbf{\Phi}_{1e}'^T + r_{11}\mathbf{v}_1^T + \mathbf{w}_1^T + m_{ac1}(r_{11} + l_{ac1})\mathbf{\Phi}_{1ac}^T$

$+ (\tfrac{1}{2}m_{21}r_{21} + m_{22}(l_2 + r_{21} + \tfrac{1}{2}r_{22})(\mathbf{\Phi}_{1e}^T + (l_1 + r_{11} + 2r_{12})\mathbf{\Phi}_{1e}'^T) + m_p(l_2 + r_{21} + r_{22}) + m_2 r_{21} + m_2 d_2)$

$\mathbf{M_{14}} = (J_{22} + J_p)\mathbf{\Phi}_{2e}'^T + m_p(l_2 + r_{21} + r_{22})(\mathbf{\Phi}_{2e}^T + r_{22}\mathbf{\Phi}_{2e}'^T) + m_{22}(l_2 + r_{21} + \tfrac{1}{2}r_{22})(\mathbf{\Phi}_{2e}^T + \tfrac{1}{2}r_{22}\mathbf{\Phi}_{2e}'^T) + r_{21}\mathbf{v}_2^T + \mathbf{w}_2^T$

$+ (l_1 + r_{11} + r_{12})(m_p(\mathbf{\Phi}_{2e}^T + r_{22}\mathbf{\Phi}_{2e}'^T) + m_{22}(\mathbf{\Phi}_{2e}^T + \tfrac{1}{2}r_{22}\mathbf{\Phi}_{2e}'^T) + \mathbf{v}_2^T) + m_{ac2}(r_{11} + l_1 + r_{12} + r_{21} + l_{ac2})\mathbf{\Phi}_{2ac}^T$

$M_{22} = J_{21} + J_{22} + J_{h2} + J_p + \tfrac{1}{4}m_{21}r_{21}^2 + m_{22}(l_2 + r_{21} + \tfrac{1}{2}r_{22})^2 + m_p(l_2 + r_{21} + r_{22})^2 + m_2 r_{21}^2 + 2m_2 d_2 r_{21} + J_{o2}$

$+ m_{ac2}(r_{21} + l_{ac2})^2$

$\mathbf{M_{23}} = (\mathbf{\Phi}_{1e}^T + r_{12}\mathbf{\Phi}_{1e}'^T).(\tfrac{1}{2}m_{21}r_{21} + m_p(l_2 + r_{21} + r_{22}) + m_{22}(l_2 + r_{21} + \tfrac{1}{2}r_{22}) + m_2 r_{21} + m_2 d_2)$

$+ (J_{21} + J_{22} + J_{h2} + J_p + J_{o2} + \tfrac{1}{4}m_{21}r_{21}^2 + m_p(l_2 + r_{21} + r_{22})^2 + m_{22}(l_2 + r_{21} + \tfrac{1}{2}r_{22})^2 + m_2 r_{21}^2 + 2m_2 d_2 r_{21})\mathbf{\Phi}_{1e}'^T$

$+ m_{ac2}(r_{21} + l_{ac2})(\mathbf{\Phi}_{1e}^T + (r_{12} + r_{21} + l_{ac2})\mathbf{\Phi}_{1e}'^T)$

$$\mathbf{M}_{24} = (J_{22} + J_p)\mathbf{\Phi}'^T_{2e} + m_{22}(l_2 + r_{21} + \tfrac{1}{2} r_{22})(\mathbf{\Phi}^T_{2e} + \tfrac{1}{2} r_{22}\mathbf{\Phi}'^T_{2e}) + m_p(l_2 + r_{21} + r_{22})(\mathbf{\Phi}^T_{2e} + r_{22}\mathbf{\Phi}'^T_{2e}) + r_{21}\mathbf{v}^T_2 + \mathbf{w}^T_2$$

$$+ m_{ac2}(r_{21} + l_{ac2})\mathbf{\Phi}^T_{2ac}$$

$$\mathbf{M}_{33} = (J_{12} + J_{21} + J_{22} + J_{h12} + J_{h2} + J_p + J_{o2} + m_2 r_{21}^2 + 2m_2 d_2 r_{21})\mathbf{\Phi}'_{1e}\mathbf{\Phi}'^T_{1e}$$

$$+ m_{12}(\mathbf{\Phi}_{1e} + \tfrac{1}{2} r_{12}\mathbf{\Phi}'_{1e})(\mathbf{\Phi}^T_{1e} + \tfrac{1}{2} r_{12}\mathbf{\Phi}'^T_{1e}) + (m_{21} + m_{22} + m_h + m_p + m_2)(\mathbf{\Phi}_{1e} + r_{12}\mathbf{\Phi}'_{1e})(\mathbf{\Phi}^T_{1e} + r_{12}\mathbf{\Phi}'^T_{1e})$$

$$+ (\tfrac{1}{4} m_{21} r_{21}^2 + m_p(l_2 + r_{21} + r_{22})^2 + m_{22}(l_2 + r_{21} + \tfrac{1}{2} r_{22})^2)\mathbf{\Phi}'_{1e}\mathbf{\Phi}'^T_{1e} + \mathbf{Z}_1$$

$$+ (\mathbf{\Phi}'_{1e}\mathbf{\Phi}^T_{1e} + \mathbf{\Phi}_{1e}\mathbf{\Phi}'^T_{1e} + 2r_{12}\mathbf{\Phi}'_{1e}\mathbf{\Phi}'^T_{1e}).(\tfrac{1}{2} m_{21} r_{21} + m_p(l_2 + r_{21} + r_{22}) + m_{22}(l_2 + r_{21} + \tfrac{1}{2} r_{22}) + m_2 r_{21} + m_2 d_2)$$

$$+ m_{ac1}\mathbf{\Phi}_{1ac}\mathbf{\Phi}^T_{1ac} + m_{ac2}(\mathbf{\Phi}_{1e} + (r_{12} + r_{21} + l_{ac2})\mathbf{\Phi}'_{1e})(\mathbf{\Phi}^T_{1e} + (r_{12} + r_{21} + l_{ac2})\mathbf{\Phi}'^T_{1e})$$

$$\mathbf{M}_{34} = (J_{22} + J_p)\mathbf{\Phi}'_{1e}\mathbf{\Phi}'^T_{2e} + m_p(l_2 + r_{21} + r_{22})\mathbf{\Phi}'_{1e}(\mathbf{\Phi}^T_{2e} + r_{22}\mathbf{\Phi}'^T_{2e}) + m_{22}(l_2 + r_{21} + \tfrac{1}{2} r_{22})\mathbf{\Phi}'_{1e}(\mathbf{\Phi}^T_{2e} + \tfrac{1}{2} r_{22}\mathbf{\Phi}'^T_{2e})$$

$$+ \mathbf{\Phi}'_{1e}(r_{21}\mathbf{v}^T_2 + \mathbf{w}^T_2) + (\mathbf{\Phi}_{1e} + r_{12}\mathbf{\Phi}'_{1e})(m_p(\mathbf{\Phi}^T_{2e} + r_{22}\mathbf{\Phi}'^T_{2e}) + m_{22}(\mathbf{\Phi}^T_{2e} + \tfrac{1}{2} r_{22}\mathbf{\Phi}'^T_{2e}) + \mathbf{v}^T_2)$$

$$+ m_{ac2}(\mathbf{\Phi}_{1e} + (r_{12} + r_{21} + l_{ac2})\mathbf{\Phi}'_{1e})\mathbf{\Phi}^T_{2ac}$$

$$\mathbf{M}_{44} = (J_{22} + J_p)\mathbf{\Phi}'_{2e}\mathbf{\Phi}'^T_{2e} + m_{22}(\mathbf{\Phi}_{2e} + \tfrac{1}{2} r_{22}\mathbf{\Phi}'_{2e})(\mathbf{\Phi}^T_{2e} + \tfrac{1}{2} r_{22}\mathbf{\Phi}'^T_{2e}) + m_p(\mathbf{\Phi}_{2e} + r_{22}\mathbf{\Phi}'_{2e})(\mathbf{\Phi}^T_{2e} + r_{22}\mathbf{\Phi}'^T_{2e})$$

$$+ \mathbf{Z}_2 + m_{ac2}\mathbf{\Phi}_{2ac}\mathbf{\Phi}^T_{2ac}$$

$$\mathbf{K}_{33} = \int_0^{l_1} EI_1 \frac{\partial^2 \mathbf{\Phi}_1}{\partial x_1^2} \frac{\partial^2 \mathbf{\Phi}_1^T}{\partial x_1^2} dx_1 \quad , \quad \mathbf{K}_{44} = \int_0^{l_2} EI_2 \frac{\partial^2 \mathbf{\Phi}_2}{\partial x_2^2} \frac{\partial^2 \mathbf{\Phi}_2^T}{\partial x_2^2} dx_2$$

We consider the constant parameters of mechanical properties: $m_i = \int_0^{l_i} \rho_i dx_i = \rho_i l_i$, $m_i d_i = \int_0^{l_i} \rho_i x_i dx_i = \tfrac{1}{2} m_i l_i$,

$J_{oi} = \int_0^{l_i} \rho_i x_i^2 dx_i = \tfrac{1}{3} m_i l_i^2$, $\mathbf{v}_i = \int_0^{l_i} \rho_i \mathbf{\Phi}_i dx_i$, $\mathbf{w}_i = \int_0^{l_i} \rho_i x_i \mathbf{\Phi}_i dx_i$, $\mathbf{Z}_i = \int_0^{l_i} \rho_i \mathbf{\Phi}_i \mathbf{\Phi}_i^T dx_i$, and $\mathbf{\Phi}_{iac} = \mathbf{\Phi}_i |_{x_i = l_{aci}}$.

Matrix $\mathbf{M}(\mathbf{q}) = \mathbf{M}_a + \mathbf{M}_b \cos(\theta_2)$ is symmetric and has part multiplied by $\cos(\theta_2)$, $\mathbf{K}$ is linear, and $\mathbf{h}(\mathbf{q}, \dot{\mathbf{q}}) = \mathbf{h}_a(\mathbf{q}, \dot{\mathbf{q}})\sin(\theta_2)$ has all terms multiplied by $\sin(\theta_2)$. Linearization around $\mathbf{q} = \mathbf{0}$ leads to $\mathbf{M} = \mathbf{M}_a + \mathbf{M}_b$ and $\mathbf{h} = \mathbf{0}$.

Shape equations ϕ_{ij}.

The deflection is separate in time and space in Eq. (21). Each flexible link may be modeled as Euler-Bernoulli beam satisfying the equation:

$$EI_i \frac{\partial^4 y_i(x_i, t)}{\partial x_i^4} + \rho_i \frac{\partial^2 y_i(x_i, t)}{\partial t^2} = 0 \tag{A1}$$

Proper boundary conditions are imposed at the base and end of each link. The link inertia is much smaller than lumped bodies inertias, so it is reasonable to assume each link constrained at the base (De Luca and Siciliano, 1991). Boundary conditions at end of each link consider the balance of bending moment and shear force:

$$y_i(0, t) = 0 \tag{A2}$$

$$y_i'(0, t) = 0 \tag{A3}$$

$$EI_i \frac{\partial^2 y_i(x_i, t)}{\partial x_i^2}\bigg|_{x_i = l_i} = -J_{Li} \frac{d^2}{dt^2}\left(\frac{\partial y_i(x_i, t)}{\partial x_i}\bigg|_{x_i = l_i}\right) - (MD)_i \frac{d^2}{dt^2}\left(y_i(x_i, t)\big|_{x_i = l_i}\right) \tag{A4}$$

$$EI_i \frac{\partial^3 y_i(x_i, t)}{\partial x_i^3}\bigg|_{x_i = l_i} = M_{Li} \frac{d^2}{dt^2}\left(y_i(x_i, t)\big|_{x_i = l_i}\right) + (MD)_i \frac{d^2}{dt^2}\left(\frac{\partial y_i(x_i, t)}{\partial x_i}\bigg|_{x_i = l_i}\right) \tag{A5}$$

Where $\quad J_{L1} = J_{12} + m_{12}(\frac{1}{2} r_{12})^2 + J_{h12} + J_{h2} + m_h r_{12}^2 J_{21} + m_{12}(\frac{1}{2} r_{12})^2 + J_p + m_p l_2^2$, $\quad J_{L2} = J_p$, $\quad M_{L2} = m_p + m_{22}$, and $M_{L1} = m_{12} + m_h + m_{21} + m_2 + m_{22} + m_p$. We consider $(MD)_i = 0$.

Generalized coordinates $\delta_{ij}(t)$ can be redefined as:

$$\delta_{ij}(t) = \exp(j\omega_{ij}t) \tag{A6}$$

Solutions for shape equations $\phi_{ij}(x_i)$ are derived from the Euler-Bernoulli beam equation (A1) and from (20) and (A6):

$$\phi_{ij}(x_i) = C_{1,ij} \sin(\beta_{ij} x_i) + C_{2,ij} \cos(\beta_{ij} x_i) + C_{3,ij} \sinh(\beta_{ij} x_i) + C_{4,ij} \cosh(\beta_{ij} x_i) \tag{A7}$$

Where $\beta_{ij}^4 = \omega_{ij}^2 \rho_i / EI_i$. Applying boundary conditions eq. (A2)-(A3) to (A7) leads to:

$$C_{3,ij} = -C_{1,ij} \ , \ C_{4,ij} = -C_{2,ij} \tag{A8}$$

Mass boundary conditions (A4)-(A5) applied to (A7) lead to an equation system (A9).

$$\left[\mathbf{F}(\beta_{ij})\right]\begin{bmatrix} C_{1,ij} \\ C_{2,ij} \end{bmatrix} = 0 \tag{A9}$$

Non-null solutions for $C_{1,ij}$, $C_{2,ij}$ are only possible if determinant of (2x2) matrix $\mathbf{F}(\beta_{ij})$ is null, leading to frequency equation (A10). There are considered the first n_i solutions for β_{ij} and $(MD)_i = 0$.

$$\left(1 + \cos(\beta_{ij}l_i)\cosh(\beta_{ij}l_i)\right) - \frac{M_{Li}\beta_{ij}}{\rho_i}\left(\sin(\beta_{ij}l_i)\cosh(\beta_{ij}l_i) - \cos(\beta_{ij}l_i)\sinh(\beta_{ij}l_i)\right)$$
$$-\frac{J_{Li}\beta_{ij}^3}{\rho_i}\left(\sin(\beta_{ij}l_i)\cosh(\beta_{ij}l_i) + \cos(\beta_{ij}l_i)\sinh(\beta_{ij}l_i)\right) + \frac{M_{Li}J_{Li}\beta_{ij}^4}{\rho_i^2}\left(1 - \cos(\beta_{ij}l_i)\cosh(\beta_{ij}l_i)\right) = 0 \tag{A10}$$

Remaining constants $C_{1,ij}$, $C_{2,ij}$ are found using Eq. (A9) depending on a scale factor. This scale factor is chosen using a suitable normalization as in Eq. (A11).

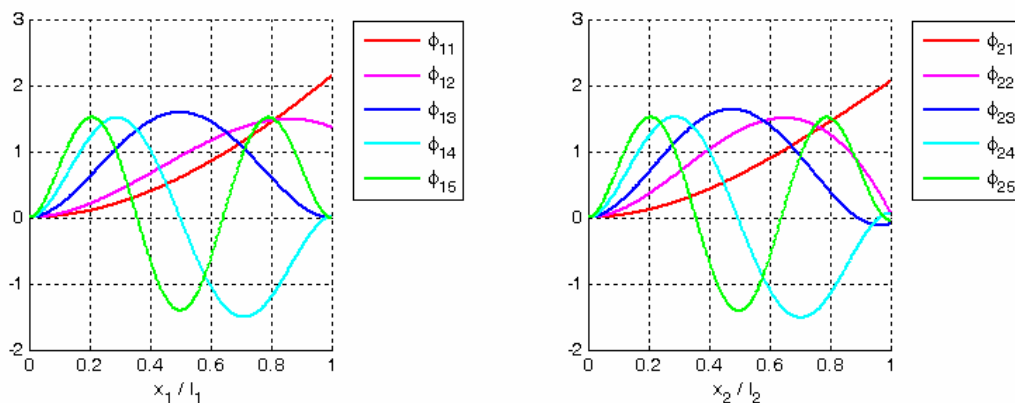$$\int_0^{l_i} \rho_i \phi_{ij}^2 dx_i = m_i \tag{A11}$$

Figure 5. Shape equations ϕ_{ij}